Dalton Transactions

Cite this: *Dalton Trans.*, 2012, **41**, 5617

www.rsc.org/dalton

PAPER

Copper(II) complexes of quinoline polyazamacrocyclic scorpiand-type ligands: X-ray, equilibrium and kinetic studies†

Carmen E. Castillo,[a] M. Angeles Máñez,[a] Manuel G. Basallote,*[a] M. Paz Clares,[b] Salvador Blasco[b] and Enrique García-España*[b]

Received 2nd February 2012, Accepted 5th March 2012
DOI: 10.1039/c2dt30223c

The formation of Cu(II) complexes with two isomeric quinoline-containing scorpiand-type ligands has been studied. The ligands have a tetraazapyridinophane core appended with an ethylamino tail including 2-quinoline (**L1**) or 4-quinoline (**L2**) functionalities. Potentiometric studies indicate the formation of stable CuL^{2+} species with both ligands, the **L1** complex being 3–4 log units more stable than the **L2** complex. The crystal structure of $[Cu(\mathbf{L1})](ClO_4)_2 \cdot H_2O$ shows that the coordination geometry around the Cu^{2+} ions is distorted octahedral with significant axial elongation; the four Cu–N distances in the equatorial plane vary from 1.976 to 2.183 Å, while the axial distances are of 2.276 and 2.309 Å. The lower stability of the $Cu\mathbf{L2}^{2+}$ complex and its capability of forming protonated and hydroxo complexes suggest a penta-dentate coordination of the ligand, in agreement with the type of substitution at the quinoline ring. Kinetic studies on complex formation can be interpreted by considering that initial coordination of **L1** and **L2** takes place through the nitrogen atom in the quinoline ring. This is followed by coordination of the remaining nitrogen atoms, in a process that is faster in the **L1** complex probably because substitution at the quinoline ring facilitates the reorganization. Kinetic studies on complex decomposition provide clear evidence on the occurrence of the molecular motion typical of scorpiands in the case of the **L2** complex, for which decomposition starts with a very fast process (sub-millisecond timescale) that involves a shift in the absorption band from 643 to 690 nm.

Introduction

Macrocyclic polyamines with appended tails including additional donor sites, which were prepared for the first time by Lotz and Kaden in 1987,[1,2] have revealed as a very interesting and broadly studied class of receptors. Later Fabbrizzi *et al.* coined these compounds with the term "scorpiand" to describe the movement performed by the tail to coordinate a metal center placed in the macrocyclic core.[3] As stated by Gokel *et al.* for mono- and bibrachial lariat crown ethers, which are analogous compounds containing oxygen donor atoms,[4,5] this class of compounds join the typical high thermodynamic stability of cryptand ligands with fast kinetics thus facilitating transport processes through organic membranes. The coordination to the metal ion of the donor atoms in the dangling arms will provide three-dimensionality to the structure preserving at the same time fast coordination dynamics. On the other hand, the analysis of the kinetics of these processes may give hints about larger scale movements and reorganizations occurring in biological systems.[6]

Within this topic, we have previously reported the acid–base and Cu^{2+} coordination chemistry of a series of ligands built up by linking together a tris(2-aminoethyl)amine unit to the 2,6 positions of a pyridine spacer through methylene groups (**L4**), and further functionalizing the hanging arm with a 1-methylnaphthyl unit (**L5**) or with 2- or 3-pycolyl groups (**L6** and **L7** in Scheme 1).[7,8] It was found that in the case of **L5**, the folding movement of the arm towards the macrocyclic core could be achieved not only by coordination of Cu^{2+} but also by formation of internal hydrogen bonds in the mono- and diprotonated forms of **L5**.[8] More recently we have reported the synthesis of two closely related ligands, **L1** and **L2**, which differ from **L6** and **L7** in that pyridine replaces quinoline.[9] The Mn(II) complexes of **L1** and **L2** show a high superoxide dismutase activity that appears to be related to the type of substitution in the dangling arm and to the structure of the complex formed. In view of these differences, we decided to carry out a detailed potentiometric and kinetic study of the corresponding Cu(II) complexes. These studies aim mainly at obtaining additional information about the effect of the substituent in the dangling arm on the solution properties of the complex.

[a]*Departamento de Ciencia de los Materiales e Ingeniería Metalúrgica y Química Inorgánica, Facultad de Ciencias, Universidad de Cádiz, Avenida República Saharahui s/n, Puerto Real, 11510 Cádiz, Spain. E-mail: manuel.basallote@uca.es*
[b]*Departamento de Química Inorgánica, Instituto de Ciencia Molecular, Universidad de Valencia, Edificio de Institutos de Paterna Apdo. 22085, 46071 Valencia, Spain. E-mail: enrique.garcia-es@uv.es*

†Electronic supplementary information (ESI) available: Tables and figures containing species distribution curves, NMR data and spectrophotometric titrations. CCDC 864923. For ESI and crystallographic data in CIF or other electronic format see DOI: 10.1039/c2dt30223c

Experimental

The synthesis of **L1** and **L2** has been described previously.[9] Crystals of [Cu**L1**]$(ClO_4)_2 \cdot H_2O$ suitable for X-ray diffraction were grown by slow evaporation of 10^{-3} M aqueous solutions of $Cu(ClO_4)_2 \cdot 6H_2O$ and L1·4HCl in the presence of an excess of $NaClO_4$ at an initial pH of 5. Unfortunately, attempts with the **L2** complex were unsuccessful. All other reagents were obtained from commercial sources.

Kinetic experiments

Depending on the time scale of the reaction, the kinetic measurements were carried out with either a Cary 50-Bio spectrophotometer or an Applied Photophysics SX17MV stopped-flow instrument provided with a PDA-1 diode array detector. In both cases, the kinetic experiments provided spectral changes with time that were analyzed with the *SPECFIT* and *ProK-II* software.[10,11] All kinetic experiments were carried out at 298.1 K using 0.15 M $NaClO_4$ as supporting electrolyte. The kinetic work on complex decomposition was carried out under pseudo-first-order conditions of acid excess and the solutions contained Cu^{2+} and the corresponding ligand in a 1 : 1 molar ratio (*ca.* 5×10^{-4} M). The pH was adjusted with NaOH to values at which the formation of the CuL^{2+} complexes in solution is complete. Complex decomposition was started by adding an excess of an $HClO_4$ solution of suitable concentration containing the required amount of $NaClO_4$ for maintaining a constant ionic strength of 0.15 M. For the kinetic studies on complex formation, a 5×10^{-4} M solution of the ligand whose pH had been previously adjusted with $HClO_4$ and NaOH was mixed in the stopped-flow instrument with a solution at the same pH and containing the same concentration of Cu^{2+}. Pseudo-first order conditions were avoided to make complexation slow enough to be measured with the stopped-flow technique and to avoid complications caused by the possibility of formation of complexes with different stoichiometries. The experiments covered a range of starting pH of 3.0–5.8. Under these conditions, complex formation can be easily monitored with the stopped-flow instrument, and Cu^{2+} initially exists almost exclusively as the aqua-complex, thus facilitating the interpretation of the kinetic data because there is not any contribution of Cu^{2+} hydroxo complexes to the net rate of complex formation. The kinetic experiments were conducted in the absence of buffer because of previous evidence showing that buffer agents can interact either with the metal ion or with the highly protonated forms of the ligand.[11–13] Although the absence of buffering agent causes significant changes in the H^+ concentration during complex formation, the problem can be solved by analysing the kinetic data with the ProK-II software,[11] which allows not only inclusion in the model fixed values of the equilibrium constants for the protonation equilibria but also a simultaneous analysis of kinetic files corresponding to experiments at different starting pH.[13] Nevertheless, kinetic models were kept as simple as possible. For that purpose, the analysis of the whole set of experiments was preceded by an individual analysis of each file using both the Specfit and ProK-II programs.[10,11,13]

Potentiometric measurements

The potentiometric titrations were carried out at 298.1 ± 0.1 K using $NaClO_4$ 0.15 M as supporting electrolyte. The experimental procedure (burette, potentiometer, cell, stirrer, microcomputer, *etc.*) has been fully described elsewhere.[14] The acquisition of the emf data was performed with the computer program PASAT.[15] The reference electrode was an Ag/AgCl electrode in saturated KCl solution. The glass electrode was calibrated as a hydrogen-ion concentration probe by titration of previously standardized amounts of HCl with CO_2-free NaOH solutions and determining the equivalent point by the Gran's method,[16,17] which gives the standard potential, $E^{\circ\prime}$, and the ionic product of water (pK_w = 13.73(1)). The computer program HYPERQUAD[18] was used to calculate the protonation and stability constants. The pH range investigated was 2.5–11.0 and the concentration of Cu^{2+} and of the ligands ranged from 1×10^{-3} to 5×10^{-3} M with M : L molar ratios varying from 2 : 1 to 1 : 2. The different titration curves for each system (at least two with over 50 experimental data points) were treated either as a single set or as separated curves without significant variations in the values of the stability constants.

NMR measurements

The ^1H and ^{13}C NMR spectra were recorded on a Bruker Avance DPX 300 MHz spectrometer operating at 299.95 MHz for ^1H and at 75.43 MHz for ^{13}C. For the ^{13}C NMR spectra, dioxane was used as a reference standard (δ = 67.4 ppm) and, for the ^1H spectra, the solvent signal. Adjustments to the desired pH were made using drops of DCl or NaOD solutions. The pD was calculated from the measured pH values using the correlation, pH = pD−0.4.[19]

Crystallographic analysis

An analysis of a single crystal of [Cu**L1**]$(ClO_4)_2 \cdot (H_2O)$ was measured in an Enraf-Nonius KappaCCD single-crystal diffractometer using MoKα radiation (λ = 0.71073 Å) at room temperature. The structure was solved with SHELXS-97 program and further refined with SHELXL-97[20] up to the final structure. Hydrogen atoms were placed in calculated positions. Final drawings of the structures were made with the Mercury program.[21]

Spectrofluorimetric measurements

The solvents used were of spectroscopic or equivalent grade. Water was twice distilled and passed through a Millipore apparatus. All solutions were prepared 0.15 mol dm^{-3} in $NaClO_4$. The pH values were measured with a Mettler-Toledo MP-120 pH-meter and adjustments of the hydrogen ion concentration of the solutions were made with diluted HCl and NaOH solutions. UV-Vis absorption spectra were recorded on Agilent 8453 spectroscopy system. The emission spectra were recorded with a PTI MO-5020 spectrofluorimeter in the 300–500 nm range with excitation wavelength of 316 nm. The absorbance was smaller than 0.1 units at the excitation wavelength.

Table 1 Stepwise protonation constants of **L1** and **L2** determined at 298.1 ± 0.1 K in 0.15 M $NaClO_4$[9]

Reaction[a]	L1	L2
$L + H \leftrightarrows HL$	10.03(1)[b]	9.93(1)
$HL + H \leftrightarrows H_2L$	8.40(1)	8.31(1)
$H_2L + H \leftrightarrows H_3L$	6.23(1)	5.94(1)
$H_3L + H \leftrightarrows H_4L$	1.93(2)[c]	2.82(1)

[a] Charges omitted for clarity. [b] Values in parenthesis are standard deviations in the last significant figure. [c] This work, determined by UV-Vis measurements.

Results and discussion

Acid–base behaviour of L1 and L2

A collection of the potentiometrically determined protonation constants and the NMR spectra of solutions containing both ligands at different pH has been previously reported,[9] but some discussion of those results is required in the context of the present work to help to a better understanding of the kinetic properties of these systems. Table 1 shows the stepwise protonation constants of **L1** and **L2** determined in 0.15 M $NaClO_4$ at 298.1 K, and the corresponding species distribution diagrams are included in Fig. 1 and the ESI.† Both ligands present four protonation constants, the first three being much higher than the fourth one. In the case of **L1** the value of the last constant was too small to allow determination from potentiometric measurements, and UV-Vis spectroscopy has now been employed to obtain an accurate value. The observed spectral changes during the titration (see Fig. S5, ESI†) show an increase of absorbance at the lowest pH values (less than *ca.* 2.5) both in the 300–350 nm and 235–245 nm ranges, which clearly support that the fourth protonation occurs at the quinoline nitrogen. Actually, similar spectral changes have been reported for other quinoline-containing molecules undergoing protonation of the quinolinic nitrogen.[22,23] Similar absorbance changes are observed for **L2** (see Fig. S6, ESI†), but they occur at higher pH values, in agreement with the potentiometric results.

Taking into account the basicity in water of the different types of nitrogen atoms in **L1** and **L2**, it is expected that the three first protonation steps should involve the secondary amino groups of the ligands; two of them located in the macrocyclic core and the other one in the tail. ^1H and ^{13}C NMR data at different pH values can give also indications about the protonation sequence followed by **L1** and **L2**. It is well known that upon protonation the hydrogen nuclei bound to the α-carbon and the carbon nuclei in the β position with respect to the nitrogen atoms undergoing protonation are those experiencing, respectively, the largest downfield and upfield shifts.[7] Tables S1 and S2† in the ESI summarize the shifts observed for the proton and carbon signals of the aliphatic part of both ligands (see Scheme 1 for the labelling and the ESI of ref. 9 for the original spectra). The variation of the ^1H signals of the protons H1 and H6 is particularly relevant for distinguishing between the protonation of the secondary amino groups in the macrocycle and in the pendant arm. For the case of **L1**, the data show that formation of $H\mathbf{L1}^+$ occurs with significant shift of all the aliphatic proton signals except that for

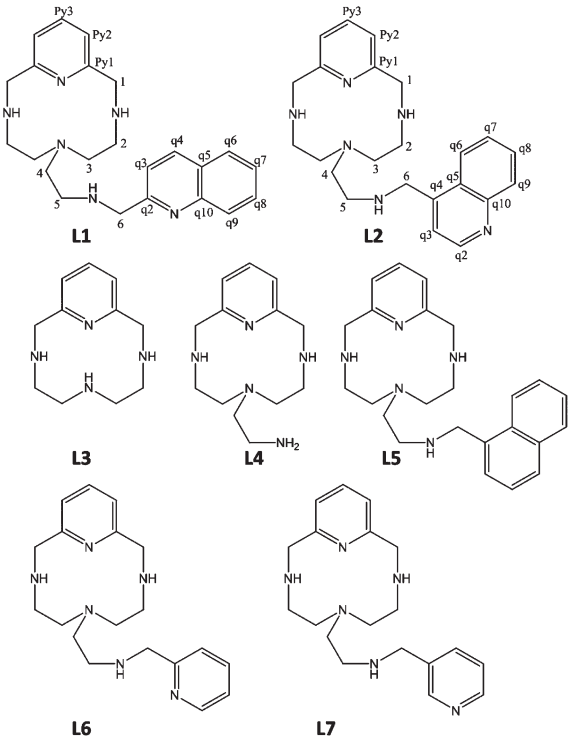

Scheme 1

H6, thus showing that the first protonation occurs at the macrocyclic ring and it surely involves formation of hydrogen bonds with participation of all the nitrogen donors in that part of the molecule. This conclusion is also supported by the shifts observed for the signals of H2, H3 and H4. In contrast, in the pH range in which second and third protonation occur, the downfield shifts for the H1 and H6 signals are both significant, thus suggesting that those protonations affect to both the macrocycle and the NH group in the pendant arm. Finally, the only signal slightly shifted upon conversion of $H_3\mathbf{L1}^{3+}$ to $H_4\mathbf{L1}^{4+}$ is that for H6, in agreement with the results from the spectrophotometric titration showing that this protonation occurs at the quinoline nitrogen. The shifts for the carbon signals in general confirm the previous conclusions from the proton spectra, it being especially relevant that the only signal that undergoes a significant upfield shift in the fourth protonation is that for C6, in agreement again with protonation at quinoline. The table in the ESI† for **L2** leads to similar conclusions, thus showing that both ligands follow a common protonation sequence in which the secondary amino groups of the macrocycle undergo protonation first, followed by the secondary amino group of the tail and by the nitrogen of the quinoline ring.

Additional information about protonation of the quinoline nitrogen was obtained in a fluorescence study. Excitation at 316 nm causes fluorescence with an emission maximum at 415 nm, the intensity of emission being strongly pH dependent. Fig. 1 shows that both $H_4\mathbf{L1}^{4+}$ and $H_3\mathbf{L1}^{3+}$ are strongly fluorescent, but emission is severely reduced under conditions in which only $H_2\mathbf{L1}^{2+}$ and less protonated species exist in solution. It is known that quinoline and its derivatives are fluorescent both in the neutral and protonated forms,[23,24] and so the results in Fig. 1 confirm that the last protonation occurs at the quinoline

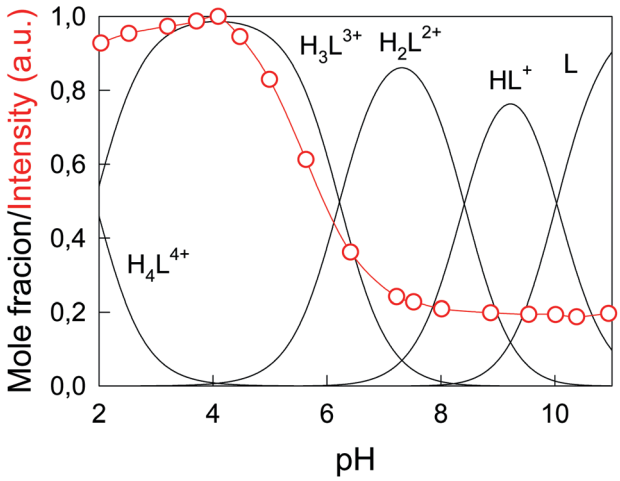

Fig. 1 Intensity of the fluorescence emission (excitation at 316 nm, emission at 415 nm) and species distribution diagrams for the protonated species of **L1**.

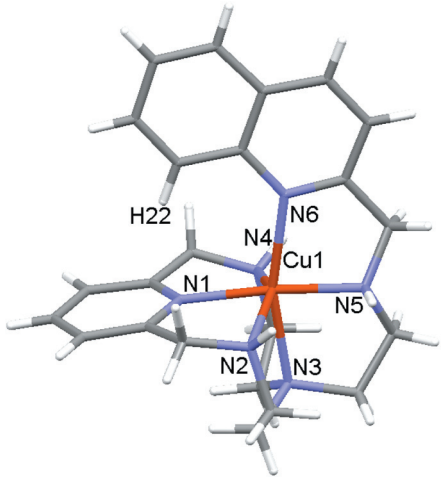

Fig. 2 Stick representation of the $[Cu(\mathbf{L1})]^{2+}$ cation. Bond distances (in Å) between the Cu1 centre and the donor atoms are 1.979(5), 2.309 (6), 2.183(6), 2.276(6), 1.976(7) and 2.173(5) for N1 to N6, respectively.

ring, in agreement with the spectrophotometric results. In the $H_3\mathbf{L1}^{3+}$ species the quinoline group would be deprotonated whereas all the remaining nitrogen atoms would be either protonated or hydrogen bonded, so that no electron pairs on the amine groups are available for photoinduced electron-transfer fluorescence quenching.[25,26] Deprotonation of $H_3\mathbf{L1}^{3+}$ involves the secondary amino group closest to the quinoline and leads to fluorescence quenching. For the case of **L2**, the results are more complex, with changes in both the intensity and the position of the maximum of emission with pH, and so no clear conclusions could be obtained.

Crystal structure of $[Cu(L1)](ClO_4)_2{\cdot}H_2O$

The asymmetric unit of $[Cu(\mathbf{L1})](ClO_4)_2{\cdot}H_2O$ is formed by one $[Cu(\mathbf{L1})]^{2+}$ cation, two perchlorate counter-ions and a lattice water molecule. The coordination geometry around the Cu^{2+} ions is distorted octahedral with significant axial elongation (see Fig. 2) as was already observed in the case of the analogous complex of the ligand **L6**, $[Cu(\mathbf{L6})](ClO_4)_2$.[7] The equatorial plane of the octahedron is defined by the pyridine and quinoline nitrogens (N1 and N6, respectively), the tertiary amino group of the ligand (N3) and the amino group of the tail (N5). The shortest distances are those with the pyridine nitrogen and the secondary amino group of the tail. The elongated axial positions are occupied by the secondary amino groups of the macrocyclic core (N2 and N4). Such a distortion is somehow dictated by the presence of the aromatic spacer that prevents a closer approach to the metal of the secondary atoms of the macrocycle. The angles in the coordination sphere vary from 78.8 to 104° (see Table S3† in the ESI). Another interesting aspect in this structure is the occurrence of a CH···π (T-shaped configuration) interaction between the quinoline and pyridine rings. The distance between the centroid of the pyridine ring and the proton of C22 in the quinoline ring is 2.76 Å.[27–29] The angle between the planes of the aromatic rings is 88.6°. However, it has to be emphasized that this disposition of the rings is somewhat imposed by the hexacoordination of the metal ion.

Table 2 Stability constants for the formation of Cu^{2+} complexes of **L1** and **L2**. Determined in $NaClO_4$ 0.15 M at 298.0 ± 0.1 K

Cu(II)		
Reaction	**L1**	**L2**
$M + L \leftrightarrows ML$[a]	21.35(1)[b]	17.66(1)
$M + L + H \leftrightarrows MHL$		21.32(2)
$M + L + H_2O \leftrightarrows ML(OH) + H$		7.64(3)
$M + L + 2H_2O \leftrightarrows ML(OH)_2 + 2H$		−4.12(8)
$ML + H \leftrightarrows MHL$		3.66(1)
$ML + OH^- \leftrightarrows ML(OH)$		3.71(1)
$ML(OH) + OH^- \leftrightarrows ML(OH)_2$		1.96(3)

[a] Charges omitted for clarity. [b] Values in parenthesis are standard deviations in the last significant figure.

Potentiometric studies on the formation of Cu(II) complexes

The analysis of the potentiometric data for the formation of Cu^{2+} complexes with both ligands leads to the equilibrium model and stability constants collected in Table 2. For the Cu^{2+}–**L1** system just a $[Cu\mathbf{L1}]^{2+}$ species of very high stability is formed. This species is completely formed at pH values as low as 3 and persists as the only species in solution for all the pH range covered. The formation constant of the $[Cu\mathbf{L1}]^{2+}$ species is quite close to that found for the related **L6** ligand,[7] which suggests a similar hexa-coordination binding mode in both cases. Therefore, the hexa-coordination observed in the crystal structure is kept in solution even in basic conditions, as confirmed by the absence of hydroxylated species.

In the case of **L2**, in addition to the $[Cu\mathbf{L2}]^{2+}$ species, the formation of a protonated, $[CuH\mathbf{L2}]^{3+}$, and two hydroxylated, $[Cu\mathbf{L2}(OH)]^{+}$ and $[Cu\mathbf{L2}(OH)_2]$, species is observed. The stability of the $[Cu\mathbf{L2}]^{2+}$ complex is lower than that of $[Cu\mathbf{L1}]^{2+}$, thus reflecting the unavailability of the quinoline nitrogen to reach the coordination sphere of the metal ion when the other donor atoms in the ligand are coordinated. Moreover, the value

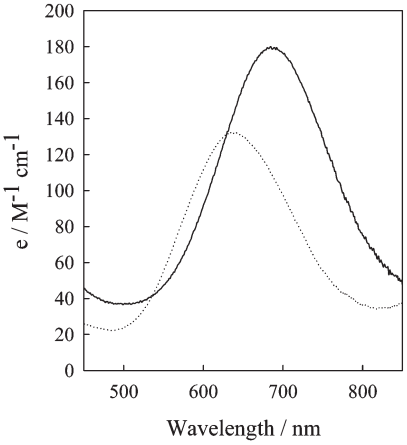

Fig. 3 Electronic spectra for aqueous solutions containing the $[Cu\mathbf{L1}]^{2+}$ (continuous line) and $[Cu\mathbf{L2}]^{2+}$ (dotted line) species at concentration 5×10^{-4} M in 0.15 M $NaClO_4$ at 298.1 K.

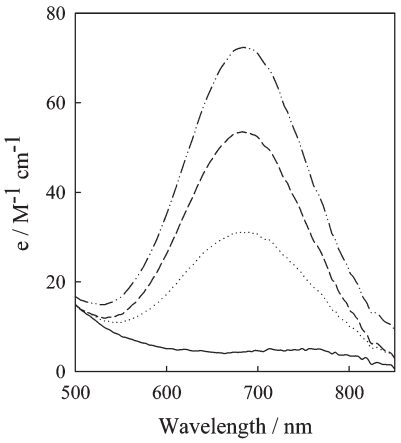

Fig. 4 Electronic spectra calculated from kinetic data for the different species involved in the formation of $[Cu\mathbf{L1}]^{2+}$; Cu^{2+} (continuous line), $HCu\mathbf{L1}^{3+}$ (dotted line), $(Cu\mathbf{L1}^{2+})_{I}$ (dashed line), $(Cu\mathbf{L1}^{2+})_{II}$ (dash-dot-dotted line), in 0.15 M $NaClO_4$ at 298.1 K.

of the stability constant obtained is even lower than those obtained for related macrocycles in which penta-coordination of the metal ion was ascertained from crystallographic data ($[Cu\mathbf{L4}]^{2+}$, log K = 20.43; $[Cu\mathbf{L5}]^{2+}$, log K = 19.65),[8] and it is close to that reported for the Cu^{2+} complex of the tetradentate macrocyclic core ($[Cu\mathbf{L3}]^{2+}$, log K = 17.78),[8] which could be even considered evidence that the secondary nitrogen in the tail does not coordinate. However, it has to be recalled that deriving coordination numbers just from these equilibrium values could be misleading, and actually the crystal structure of the related $[Mn\mathbf{L2}(H_2O)](ClO_4)_2$ complex shows a penta-dentate coordination of the ligand with the quinoline ring placed far away from the metal atom.[7] In any case, whatever the ligand acts as tetra- or penta-dentate, the nitrogen atom in the quinoline ring can be protonated to form a $[CuH\mathbf{L2}]^{3+}$ species and additional positions in the coordination sphere can be used for the formation of the hydroxylated species.

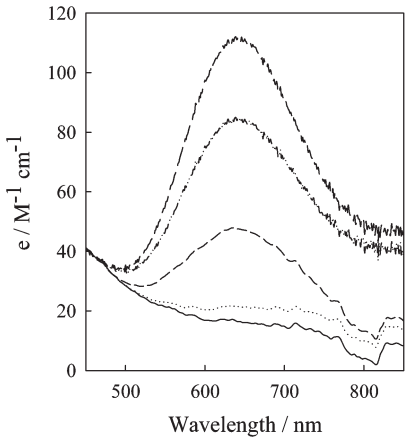

Fig. 5 Electronic spectra of the species involved in the formation of $[Cu\mathbf{L2}]^{2+}$; Cu^{2+} (continuous line), $HCu\mathbf{L2}^{3+}$ (dotted line), $(Cu\mathbf{L2}^{2+})_{I}$ (dashed line), $(Cu\mathbf{L2}^{2+})_{II}$ (dash-dot-dottd line), $(Cu\mathbf{L2}^{2+})_{III}$ (long-dashed line) in 0.15 M $NaClO_4$ at 298.1 K.

Kinetics of formation of the Cu(II) complexes

For both ligands, experiments on complex formation using the diode array detector allowed the observation of spectral changes typical for complex formation according to eqn (1), the final spectra showing an absorption maximum at 683 nm for **L1** and 640 nm for **L2**, in agreement with the spectra observed for solutions containing the corresponding CuL^{2+} species (Fig. 3–5). However, for both ligands the reaction occurs with several kinetically resoluble steps, three consecutive steps for **L1** (eqn (2)–(4)) and four steps for **L2** (eqn (2)–(5)). Because of the non-pseudo first order conditions used in the experiments, kinetic models used for data analysis always included a first step showing a first order dependence with respect to each one of the reagents, the metal ion and the ligand. The contribution of the different protonated forms of the ligand was deduced from the pH-dependence of the kinetic data by using different kinetic models. It is interesting to note that for both ligands the analysis of individual files at different pH and the global fitting of the whole set of data for a given ligand indicates that the only form which contributes to complex formation is H_3L^{3+}. The absence of contribution from H_4L^{4+} can be easily understood not only because of its lower concentration with respect to the tri-protonated form in that pH range, but also because from an electrostatic point of view, its interaction with the cationic metal ion will be less favoured than with H_3L^{3+}. The negligible contribution of H_2L^{2+} is more surprising, but inspection of the species distribution curves indicates that H_2L^{2+} reaches a maximum of *ca.* 15–20% of the total ligand species at the highest pH values covered in the kinetic studies, so that in order to discriminate between the contributions of the di- and tri-protonated species, the rate constant for reaction between Cu^{2+} and H_2L^{2+} should be at least about one order of magnitude faster than with H_3L^{3+}. As no contribution from H_2L^{2+} can be distinguished, it must be concluded that the rate constants for reaction of Cu^{2+} with the H_2L^{2+} and H_3L^{3+} species are not very different despite the change in the charge. This conclusion can be rationalized by invoking the information offered by the ^{1}H-NMR spectra at different pH. These experiments revealed that in the H_2L^{2+} species all the secondary amino groups in the

macrocycle and in the pendant arm are either protonated or involved in hydrogen bonds with other protonated amino groups, which leads to a closed structure of the ligand in which those donor groups are ineffective for the coordination to the metal center. Although the importance of the network of hydrogen bonds in the protonated forms of these ligands has been previously demonstrated,[7,8] it is interesting to note that in the case of **L6** and **L7** the protonated form of the ligand able to lead to complex formation with Cu^{2+} in moderately acidic solutions is different, H_3L^{3+} for **L6** and H_2L^{2+} for **L7**, whereas for **L1** and **L2** it is always the tri-protonated species which leads to complex formation. These results make clear that anticipating the nature of the ligand species kinetically active in the complexation processes is very difficult because the actual hydrogen bond network is different for every ligand and even for each protonated form.

$$Cu^{2+} + H_xL^{x+} \rightarrow CuL^{2+} + xH^+ \quad (1)$$

$$Cu^{2+} + H_3L^{3+} \rightarrow HCuL^{3+} + 2H^+ \quad (2)$$

$$HCuL^{3+} \rightarrow (CuL^{2+})_I + H^+ \quad (3)$$

$$(CuL^{2+})_I \rightarrow (CuL^{2+})_{II} \quad (4)$$

$$(CuL^{2+})_{II} \rightarrow (CuL^{2+})_{III} \quad (5)$$

With regard to the numerical values of the rate constants and the processes occurring at each kinetic step, the first step in the case of **L1** probably corresponds to formation of a protonated form of the complex with a second order rate constant of $(4.7 \pm 0.2) \times 10^3$ M^{-1} s^{-1}, and this intermediate is deprotonated in a second step with a rate constant of $(1.50 \pm 0.04) \times 10^{-1}$ s^{-1}. The last step is a reorganization process with a rate constant of $(1.60 \pm 0.01) \times 10^{-2}$ s^{-1}. Unfortunately, the spectra calculated from kinetic data for the different intermediates (Fig. 4) are not very informative and precise details of these reorganizations cannot be deduced.

In the case of **L2**, complex formation is even more complicated because it involves one additional reorganization step. In this case the analysis of the data leads to the following rate constants: $k_1 = (1.03 \pm 0.01) \times 10^4$ M^{-1} s^{-1}, $k_2 = (2.96 \pm 0.01) \times 10^{-2}$ s^{-1}, $k_3 = (8.5 \pm 0.2) \times 10^{-4}$ s^{-1} and $k_4 = (5.0 \pm 0.2) \times 10^{-5}$ s^{-1}. Because of the different timescales of the steps, the rate constants for the first two steps were derived from stopped-flow measurements and those for the last two stages from data recorded with a conventional UV-Vis spectrometer. As shown in Fig. 5, the spectral changes associated with the first step are very small and although they could be thought of as an artefact caused by some impurity or secondary process, this possibility was ruled out after careful fitting to a variety of kinetic models. Moreover, this is the only step with a first order dependence with respect to both reagents and the rate constant is close to that observed for the first step in the reaction with **L1**, which suggests that they both correspond to the formation of an H_xCuL species. A possible explanation would be that the formation of the complexes with **L1** and **L2** ligands start with the interaction of the metal centre with the donor atom in the quinoline ring, which is the most readily available donor atom in the H_3L^{3+} form of both ligands, but that species evolves in different ways for both ligands due to the difference in the position of substitution at the aromatic ring. In the case of **L1**, reorganization to an intermediate coordinated to the macrocyclic centre would be so fast that the intermediate with monodentate coordination to the quinoline nitrogen is not detected, whereas for **L2** the process is not so favoured and conversion to the next intermediate is slow enough to be kinetically resoluble. As a consequence, for the case of the **L2** ligand the intermediate with the ligand acting as monodentate is detected with a spectrum closer to that of the aquo–copper complex (Fig. 3). Additional evidence favouring this interpretation comes from the fact that numerical values of k_1 for reaction of Cu^{2+} with $H_3\mathbf{L2}^{3+}$ and $H_3\mathbf{L1}^{3+}$ are close to each other and not very different from those found for reaction with the protonated form of related ligands containing pyridyl groups in the pendant arm (**L6** and **L7**), but they are significantly faster (3–4 orders of magnitude) than reaction with protonated forms of related compounds without donor atoms in aromatic groups at the pendant arm (**L4** and **L5**). In the latter cases the reaction is expected to be forced to proceed through interaction of the metal ion with the macrocycle or the NH group at the pendant arm, and all donor groups in that part of the molecule are either protonated or involved in hydrogen bonds.

Kinetics of decomposition of the Cu(II) complexes

In general, addition of an excess of acid to solutions containing metal–polyamine complexes results in complex decomposition according to eqn (6). However, in the case of $Cu\mathbf{L2}^{2+}$ the spectra obtained immediately after mixing display a maximum shifted from 643 nm (reference, unreacted complex) to 690 nm (Fig. 6a). This reveals the existence of an initial step, too fast for the stopped-flow technique, that leads to a species with a spectrum similar to that observed for **L1**. The process takes place within the mixing time of the instrument (*ca.* 1.7 ms) even at very low concentration of acid. Following this initial step, there is complete decomposition of the complex (see Fig. 6b), in a slow process that was monitored with conventional UV-Vis spectrophotometry. The spectral changes were fitted satisfactorily by a single exponential to obtain k_{obs} values that show a linear dependence with respect to the acid concentration (eqn (7)) with $a = (6.0 \pm 0.2) \times 10^{-4}$ M^{-1} s^{-1}.

$$CuL^{2+} + H^+_{exc} \rightarrow Cu^{2+} + H_xL^{x+} \quad (6)$$

$$k_{obs} = a[H^+] \quad (7)$$

The initial rapid process must correspond to protonation of $Cu\mathbf{L2}^{2+}$ to form a $H_xCu\mathbf{L2}^{(2+x)+}$ species. On the basis of the equilibrium studies, this species is most likely $HCu\mathbf{L2}^{3+}$, in which the metal ion is coordinated exclusively to the four donor atoms of the macrocycle ring, a hypothesis that is further supported by the fact that $Cu\mathbf{L3}^{2+}$, which lacks of pendant arm shows a band at 695 nm.[8] Moreover, a similar shift in the position of the absorption band from *ca.* 640 to 690 nm during the mixing time has been observed previously for the copper complexes with the related scorpiand-like ligands **L4**, **L5** and **L7**, and the subsequent decomposition of the corresponding species also occurs with the rate law in eqn (7) with values of a that span over a relatively narrow range [$(3.9–9.7) \times 10^{-4}$ M^{-1} s^{-1}].[7,8]

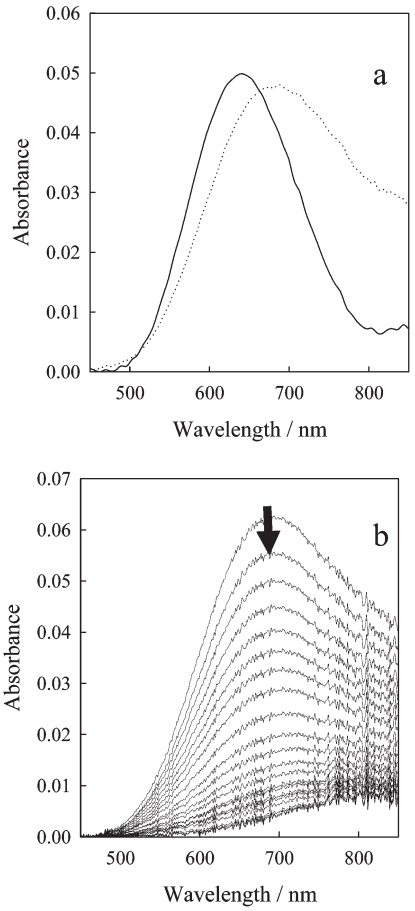

Fig. 6 (a) Electronic spectra of a solution of Cu**L2**$^{2+}$ (continuous line) and immediately (*ca.* 1.7 ms) after mixing with a diluted solution of $HClO_4$ (dotted line). (b) Spectral changes associated with the reaction of Cu**L2**$^{2+}$ with a concentrated solution of $HClO_4$. The latter changes occur in a much slower timescale that spans over *ca.* 1000 min.

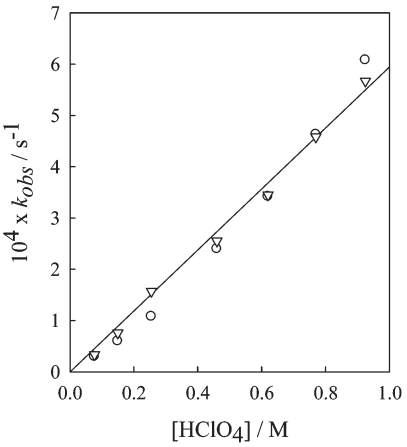

Fig. 7 Plot of the dependence on the acid concentration of the observed rate constant for the second kinetic step in the acid-promoted decomposition of the Cu**L1**$^{2+}$ (triangles) and Cu**L2**$^{2+}$ (circles) complexes ($NaClO_4$ = 0.15 M, 298.1 K). For simplicity, only the line for the best fit of both sets of data is shown.

In contrast, Cu**L1**$^{2+}$ decomposes in a single kinetic step with disappearance of the maximum at 683 nm. Decomposition is slow and the observed rate constants can be also fitted satisfactorily by eqn (7) with $a = (5.9 \pm 0.1) \times 10^{-4}$ M^{-1} s^{-1}. The similarity of the kinetic data for decomposition of Cu**L1**$^{2+}$ with those of HCu**L2**$^{3+}$ (see Fig. 7) and the **L4**, **L5** and **L7** complexes, suggests that they correspond to quite similar processes, most likely dissociation of the metal ion from a species in which it is coordinated at the macrocycle ring and the NH group in the pendant arm. However, as the equilibrium data and the crystal structure show that the dentate character of the ligand in Cu**L1**$^{2+}$ is six, a rapid step occurring before the slow one should be observed for this complex. The lack of observation of such a step indicates that it is probably masked because the intermediate is formed under steady-state conditions or it has spectral characteristics similar to those of the starting complex.

The present results can be rationalized assuming the mechanism of complex decomposition proposed by Margerum *et al.* for the decomposition of metal chelates and discussed by Lan and Chung for the case of Cu^{2+} with linear and macrocyclic polyamine ligands some years ago.[30–33] In this mechanism, there is the initial formation of an activated intermediate ($[CuL]^{2+}$)* with an elongated Cu–N bond, which is susceptible to be attacked by the solvent or a proton, as shown in eqn (8)–(10). The rate law for this mechanism is given by eqn (11) that can be reduced to the form of eqn (7) with $a = K_1k_H$. This simplification indicates that in the present case the complex decomposes exclusively through the proton-assisted pathway; *i.e.*, H_2O is not able to cause the complete breakage of the Cu–N bond in the activated intermediate. This simplification is quite common[34] and hinders derivation of any of the rate constants in eqn (8)–(10).

$$\text{M–L} \underset{}{\overset{}{\rightleftarrows}} (\text{M–L})*, k_1, k_{-1} : \; K_1 \tag{8}$$

$$\text{H}^+ + (\text{M–L})* \rightarrow \text{M} + \text{LH}, k_\text{H}, \text{H}^+ \tag{9}$$

$$\text{H}_2\text{O} + (\text{M–L})* \rightarrow \text{M} + \text{L}, k_{\text{H}_2\text{O}} \tag{10}$$

$$k_{\text{obs}} = \frac{k_1 k_{\text{H}_2\text{O}} + k_1 k_\text{H}[\text{H}^+]}{k_1 + k_{\text{H}_2\text{O}} + k_\text{H}[\text{H}^+]} \tag{11}$$

Conclusion

Despite the similar structure of the two ligands, the different substitution position of the quinoline ring leads to different properties of their Cu^{2+} complexes, which affect to the stability of the complexes and the kinetics of reaction. The stability of the Cu^{2+} complex with **L1** is higher because of the simultaneous coordination of all the nitrogen atoms, which is not possible with **L2**. Kinetic results on complex formation can be interpreted in both cases by considering that the initial coordination takes place through the quinoline nitrogen. However, whereas for **L1** this coordination acts as a bridgehead and allows fast coordination of the remaining nitrogen atoms, the different substitution in the **L2** molecule makes reorganization slower and the monodentate intermediate is detected in the kinetic studies. Kinetic studies on complex decomposition provide clear evidence on the occurrence of the molecular motion typical of scorpiands in the case of the **L2** complex, for which decomposition starts with a very

fast process (sub-millisecond timescale) that involves a shift in the absorption band from 643 to 690 nm. Probably, a similar process occurs for the **L1** complex, but the corresponding reaction intermediate would be formed under steady-state conditions in that case.

Acknowledgements

Financial support by the Spanish Ministerio de Ciencia e Innovación and FEDER funds of the E.U. (Projects CTQ2009-14443-C02-01, CTQ2009-14288-CO4-01 and CONSOLIDER INGENIO 2010 CSD2010-00065), Generalitat Valenciana (PROMETEO 2011/008) and Junta de Andalucía (Grupo FQM-137) is gratefully acknowledged.

Notes and references

1 T. J. Lotz and T. A. Kaden, *Helv. Chim. Acta*, 1978, **61** (4), 1376–1387.
2 T. J. Lotz, *J. Chem. Soc., Chem. Commun.*, 1977, 15–16.
3 P. S. Pallavicini, A. Perotti, A. Poggi, B. Seghi and L. Fabbrizzi, *J. Am. Chem. Soc.*, 1987, **109** (17), 5139–5144.
4 R. A. Schultz, D. M. Dishong and G. W. Gokel, *J. Am. Chem. Soc.*, 1982, **104** (2), 625–626.
5 D. M. Goli, D. M. Dishong, C. J. Diamond and G. W. Gokel, *Tetrahedron*, 1982, **23** (50), 5243–5246.
6 K. Kinbara and T. Aida, *Chem. Rev.*, 2005, **105** (4), 1377–1400.
7 S. Blasco, B. Verdejo, M. P. Clares, C. E. Castillo, A. Algarra, J. Latorre, M. A. Mañez, M. G. Basallote, C. Soriano and E. García-España, *Inorg. Chem.*, 2010, **49** (15), 7016–7027.
8 B. Verdejo, A. Ferrer, S. Blasco, C. E. Castillo, J. González, J. Latorre, M. A. Mañez, M. G. Basallote, C. Soriano and E. García-España, *Inorg. Chem.*, 2007, **46** (14), 5707–5719.
9 M. P. Clares, S. Blasco, M. Inclán, L. del Castillo Agudo, B. Verdejo, C. Soriano, A. Doménech, J. Latorre and E. García-España, *Chem. Commun.*, 2011, **47**, 5988–5990.
10 R. A. Binstead, B. Jung and A. D. Zuberbühler, *SPECFIT-32, Spectrum Software Associates*, Chappel Hill, 2000.
11 M. Maeder, Y. M. Neuhold, G. Puxty and P. King, *Phys. Chem. Chem. Phys.*, 2003, **5** (13), 2836–2841.
12 M. G. Basallote, J. Durán, M. J. Fernández-Trujillo, M. A. Mañez and B. Szpoganicz, *J. Chem. Soc., Dalton Trans.*, 1999 (7), 1093–1100.
13 N. McCann, G. A. Lawrance, Y. M. Neuhold and M. Maeder, *Inorg. Chem.*, 2007, **46** (10), 4002–4009.
14 E. García-España, M.-J. Ballester, F. Lloret, J. M. Moratal, J. Faus and A. Bianchi, *J. Chem. Soc., Dalton Trans.*, 1988, 101–104.
15 M. Fontanelli and M. Micheloni, *Proceedings of the I Spanish-Italian Congress on Thermodynamics of Metal Complexes*, Peñíscola, Castellon, Spain, 1990.
16 G. Gran, *Analyst*, 1952, **77**, 661–671.
17 F. J. C. Rossotti, *J. Chem. Educ.*, 1965, **42** (7), 375–378.
18 P. Gans, A. Sabatini and A. Vacca, *Talanta*, 1996, **43**, 1739.
19 A. K. Covimgton, M. Paabo, R. A. Robinson and R. G. Bates, *Anal. Chem.*, 1968, **40** (4), 700–706.
20 G. M. Sheldrick, *Acta Crystallogr., Sect. A: Found. Crystallogr.*, 2007, **64**, 112–122.
21 C. F. Macrae, I. J. Bruno, J. A. Chisholm, P. R. Edgington, P. McCabe, E. Pidcock, L. Rodriguez-Monge, R. Taylor, J. van de Streek and P. A. Wood, *J. Appl. Crystallogr.*, 2008, **41**, 466–470.
22 Y. Shiraishi, C. Ichimura and T. Hirai, *Tetrahedron Lett.*, 2007, **48** (44), 7769–7773.
23 T. C. Chien, L. G. Dias, G. M. Arantes, L. G. C. Santos, E. R. Triboni, E. L. Bastos and M. J. Politi, *J. Photochem. Photobiol., A*, 2008, **194** (1), 37–48.
24 T. Gunnlaugsson, D. A. Mac Dónaill and D. Parker, *J. Am. Chem. Soc.*, 2001, **123** (51), 12866–12876.
25 J. Herbich, M. Kijak, A. Zielinska, R. P. Thummel and J. Waluk, *J. Phys. Chem. A*, 2002, **106** (10), 2158–2163.
26 M. P. Clares, J. Aguilar, R. Aucejo, C. Lodeiro, M. T. Albelda, F. Pina, J. C. Lima, A. J. Parola, J. Pina, J. Seixas de Melo, C. Soriano and E. García-España, *Inorg. Chem.*, 2004, **43** (19), 6114–6122.
27 C. A. Hunter and J. K. M. Sanders, *J. Am. Chem. Soc.*, 1990, **112** (14), 5525–5534.
28 C. Janiak, *J. Chem. Soc., Dalton Trans.*, 2000, 3885–3896.
29 T. C. Dinadayalane and J. Leszczynski, *Struct. Chem.*, 2009, **20** (1), 11–20.
30 D. W. Margerum, G. R. Cayley, D. C. Weatherburn and G. K. Pagenkopf, *ACS Monography*, 1978, N°. **174**, 1.
31 R. A. Read and D. W. Margerum, *Inorg. Chem.*, 1981, **20** (10), 3143–3149.
32 L. H. Chen and C. S. Chung, *Inorg. Chem.*, 1989, **28** (7), 1402–1405.
33 J. H. Espenson, McGraw-Hill, 1995, 2nd edn, 102–103.
34 M. G. Basallote, J. Durán, M. J. Fernández-Trujillo and M. A. Mañez, *J. Chem. Soc., Dalton Trans.*, 1999, 3817–3823.

